MODEL STUDIES ON THE FORMATION OF INNER MORAINES IN THE ABLATION AREAS OF GLACIERS

Masayuki HASHIMOTO and Gorow WAKAHAMA

The Institute of Low Temperature Science, Hokkaido University, Kita-19, Nishi-8, Kita-ku, Sapporo 060

Abstract: Formation mechanism of inner moraines was studied in a cold laboratory near 0°C by simulation of compressing ice flow near the terminus of glaciers. For this study an apparatus was made to visualize the process of incorporation of sands into the ice mass in conjunction with two-dimensional ice flow. The results indicate the following: When a stagnant ice zone exists near the terminus, the sands are incorporated into the ice mass in the upstream side of the zone by shear action. If an obstacle exists on the bottom at this side and regelation takes place on the downstream side of the obstacle, the sands are incorporated into the ice mass immediately on the top of the regelation ice and further move obliquely upward along the flow line to the upper surface of the glacier.

1. Introduction

Debris layers called "inner moraines" (WEERTMAN, 1961) or "shear moraines" (BISHOP, 1957) are often found at the ice surface near the terminus of glaciers, ice sheets and ice caps. Field observations of the moraines of this kind were extensively carried out in the Thule area of Greenland (BISHOP, 1957; GOLDTHWAIT, 1960; SWINZOW, 1962; HOOKE, 1970), Baffin Island (GOLDTHWAIT, 1951; WARD, 1952; HOOKE, 1973), and the Antarctic ice sheet (HOLLIN and CAMERON, 1961; SOUCHEZ, 1967).

The main problem on the formation of inner moraines lies in the incorporation of debris into an ice mass at the bottom of a glacier. BISHOP (1957) proposed a hypothesis of shear mechanism. He assumed that a narrow zone is stagnant along the terminus, acting as a stagnant barrier in impeding ice movement from the interior and consequently forming shear, as an active ice mass rides over the stagnant ice zone. He assumed further that debris from the bedrock can be picked up and transported ultimately to the upper surface along shear planes. Later, SWINZOW (1962) and SOUCHEZ (1967) supported this shear hypothesis. However, WEERTMAN (1961) and HOOKE (1968) argued about Bishop's shear hypothesis on physical grounds. WEERTMAN (1961) proposed the freezing model of the incorporation of debris into the ice mass by the freezing of water in the zone near the terminus, where the ice mass ceases to slide and becomes frozen to the bedrock. However, he did not offer any field evidence to verify the model. What HOOKE (1968) suggested in his argument is that the upward movement of ice near the margin of Greenland ice sheet was caused by the movement of ice against a stagnant wind-drift ice wedge and that the boundary between such a wedge and the active ice mass was marked by a rapid, but not discontinuous decrease in shear strain downward. Later, HOOKE (1973) confirmed the validity of his suggestion by

measuring deformation of ice at the margin of Barnes Ice Cap. Furthermore, BOULTON (1970) suggested from his observation on polar glaciers in Svalbard that the debris are largely incorporated by basal freezing on the downstream sides of bedrock obstacles.

The present authors carried out simulation experiments near 0°C, using a two-dimensional model of flow in which a stagnant ice zone was formed near the terminus and an obstacle which was put at the bottom of the apparatus. The results of experiments on the stagnant ice zone and the obstacle suggested the validity of the hypothesis of shear mechanism and BOULTON's suggestion, respectively.

2. Experimental Method

2.1. Experimental apparatus

An apparatus shown in Fig. 1 was made to simulate two-dimensionally compressing flow over the bedrock near the terminus of a glacier. A mould (M) providing the space of flow, which is shaded in Fig. 1, was made of transparent acrylic acid resin and it was sandwiched between two 20 mm-thick wall plates (W) made of the same material. For securing the flow space in which the deformation of ice takes place two-dimensionally under continuous compression applied to the body of ice on the upper mouth, a steel plate (P) of 10 mm in thickness was attached to the exterior of each flat side of the sandwiched structure and all of them were fastened together tightly with bolts and nuts. The inner shape of the mould exhibited a modeled ice body near the terminus. The ice inside the mould was subjected to a constant compressive stress of 30 bar at the top surface of the upstream part (A-A'). Preparation of the ice will be described in the next subsection.

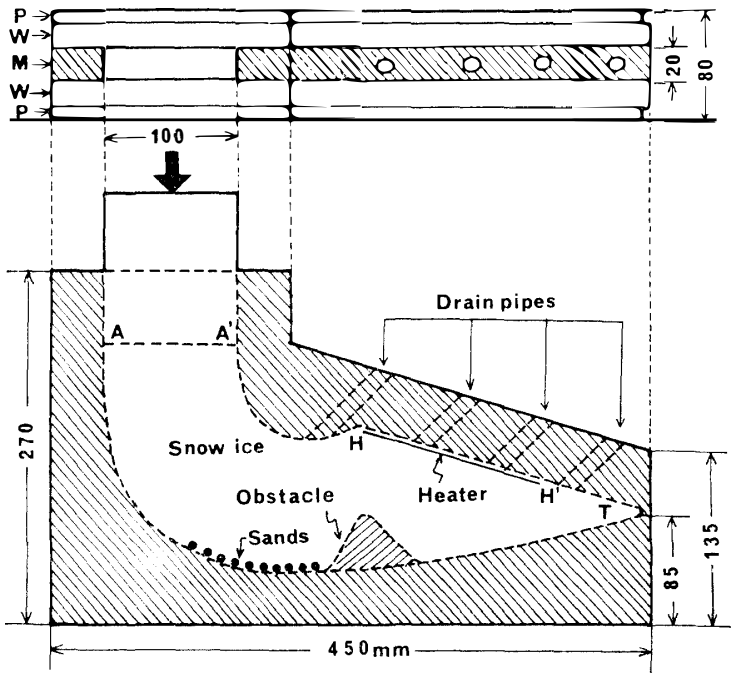

Fig. 1a. Schematic diagram of the experimental apparatus.

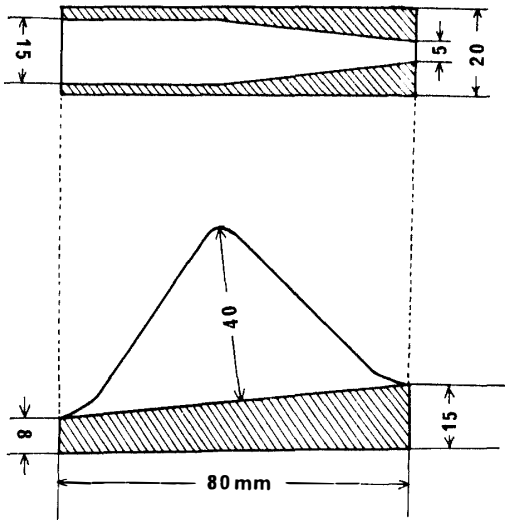

Fig. 1b. Obstacle used in the experiments which was fixed at the bottom.

For simulating the ablation of ice near the terminus, the upper surface of the ice in the mould was gradually melted by heating with an electric heater (H-H′) attached to the lower side of the upper mould. The meltwater was drained through four drain pipes perforated through the upper mould. By adjusting the supply of heat, the steady flow of ice was obtained. As the top surface (A-A′) sank under load, wet snow was supplied to the top of the opening and it turned into ice within half an hour as a result of compression.

The obstacle was made of an iron block, having a cross section of an isosceles triangle 80 mm in length of the base and 40 mm in height, as shown in Fig. 1b. The width of horizontal section of it was a little narrower than that of the mould and tapered toward the terminus, as also shown in the figure. Gaps between the obstacle and the side walls are to prevent heat conduction from outside for keeping the obstacle at the melting point of ice.

2.2. Preparation of the ice and measuring method of deformation of ice

A small amount of sands, which were sieved through a 36-mesh screen and 2.7×10^3 kg/m^3 in density, was placed in a layer 2–3 mm thick at the bottom of an ice mass, as shown in Fig. 1a. Then, the cavity of the mould was filled with snow particles sieved through a 20-mesh screen and they were soaked with distilled water at 0°C. The ice was formed in the mould when it was kept in a cold laboratory at about −10°C. The ice thus prepared contained a small amount of air bubbles and its density was 8.9×10^2 kg/m^3. The sands were supplied from time to time at the bottom of the ice mass during the experiments.

For measuring the velocity of flow and the strain-rate of ice in conjunction with the movement of sands, markings were put on the one side of the ice mass at regular grid points, as shown in Figs. 2a and 3a, as follows: After complete freezing of the ice, the wall plate of the one side was taken out; holes, 1.5 mm in diameter and 10 mm in depth, were drilled into ice; and sand particles were frozen into these holes as markers.

Before the experiment was started, the apparatus was transferred into a cold labo-

ratory at 0 ± 0.2°C and kept there for more than 12 hours for annealing. All experiments were carried out at 0 ± 0.2°C with a compressive stress of 30 bar. In the course of each experiment, photographs were taken intermittently to examine the deformation of ice and the movement of sands. The steel plates of both sides were taken off for a short time of taking photographs.

3. Experimental Results

3.1. Movement of sands from the bed

3.1.1. The case of the smooth bed

The case in which experiments are carried out without a triangular obstacle on the bottom bed of the mould is called "the case of the smooth bed". As compression proceeded, the sands moved along the bed near the terminus (Figs. 2b and 2c), from where the sands moved obliquely upward, incorporating themselves into the ice mass, and finally reached the upper surface (Fig. 2d). As seen in Fig. 2d, the accumulated sands had five peaks of undulation, which are likely to have been caused by the four consecutive additions of sands during the experiment.

3.1.2. The case of the bed with a triangular obstacle

The sands moved along the bed in the same manner as the previous case, and when the sands encountered the obstacle, they were separated into three directions: to the front slope and to both the transverse sides of the obstacle (Fig. 3b). Sand particles which climbed along the slope of the obstacle incorporated themselves into the ice mass at the top of the obstacle (Fig. 3c), forming a thin layer of sands, moved along the flow line, and finally reached the upper surface near the terminus (Fig. 3d). The sand particles which moved through narrow clearances at both sides of the obstacle gradually climbed through the medium of ice to the upper surface near the terminus (Fig. 3d).

3.2. Flow of ice

To estimate the deformation of ice quantitatively in conjunction with the movement of sands, calculations of flow velocity, principal strain-rates and principal stress deviators of ice were carried out from the observed movement of markers of grids in the ice. The velocity of each mark on the side surface of ice was obtained from the displacement vectors of the marks during the first five hours of compression. The results are shown in Figs. 4a and 5a for the case of the smooth bed and for the case with the obstacle, respectively. Assuming a two-dimensional homogeneous strain, principal strain-rates were calculated from the deformation of the grids by using NYE's formulae (NYE, 1959). The calculation results are shown in Figs. 4b and 5b for the two cases as stated above. Principal stress deviators were deduced by using GLEN's flow law of ice (GLEN, 1955). In the calculation, it is also assumed that the flow is independent of a superposed hydrostatic pressure, and that the ice is isotropic and incompressible.

The effective strain-rate $\dot{e}$ and the effective shear stress τ are defined by NYE (1953) as

$$2\dot{e}^2=\dot{\epsilon}_1^{\,2}+\dot{\epsilon}_2^{\,2}+\dot{\epsilon}_3^{\,2} \tag{1}$$

and

$$2\tau^2=\sigma_1'^2+\sigma_2'^2+\sigma_3'^2, \tag{2}$$

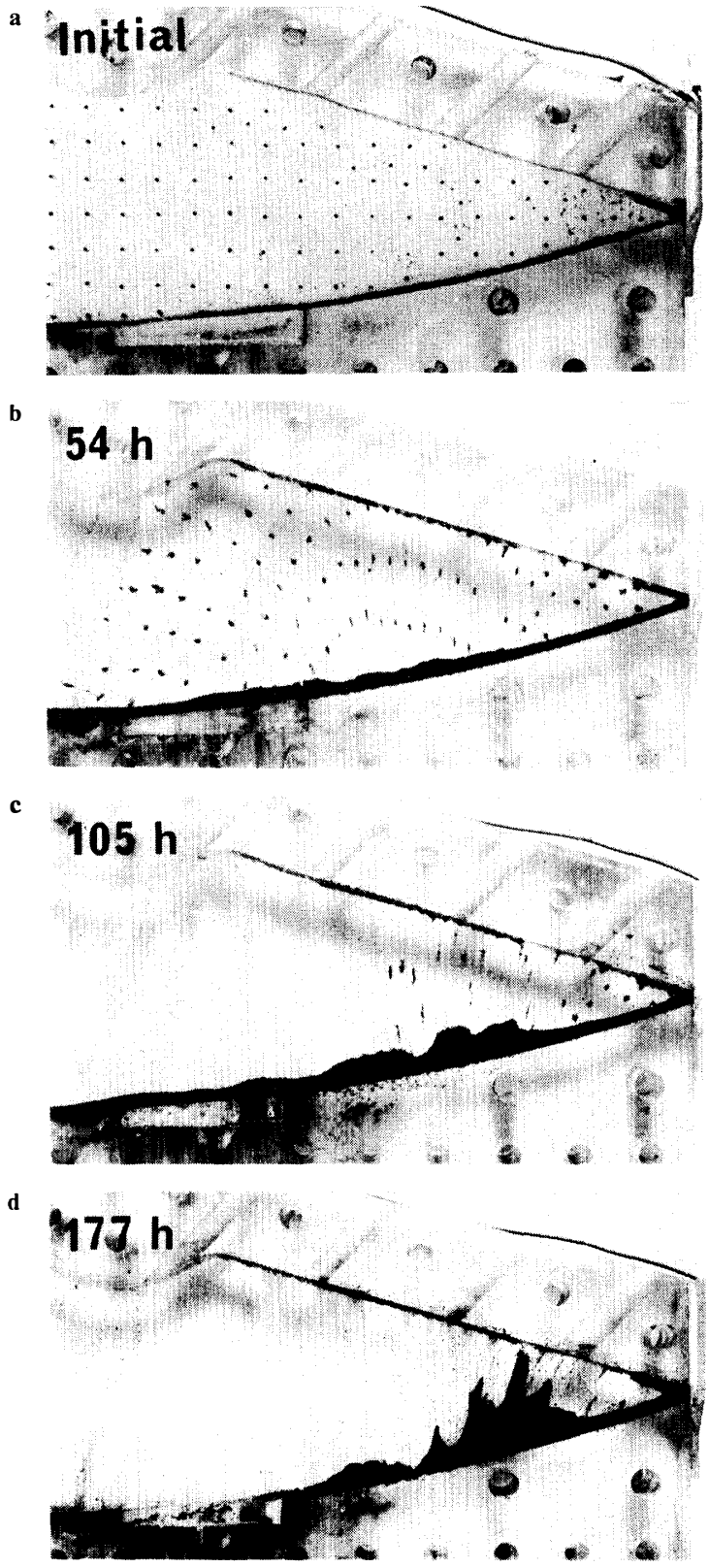

Fig. 2. Flow of ice and movement of sands in the smooth bed experiment. Longitudinal vertical section of the ice was marked with grid points to obtain the velocity and the strain rate in ice.

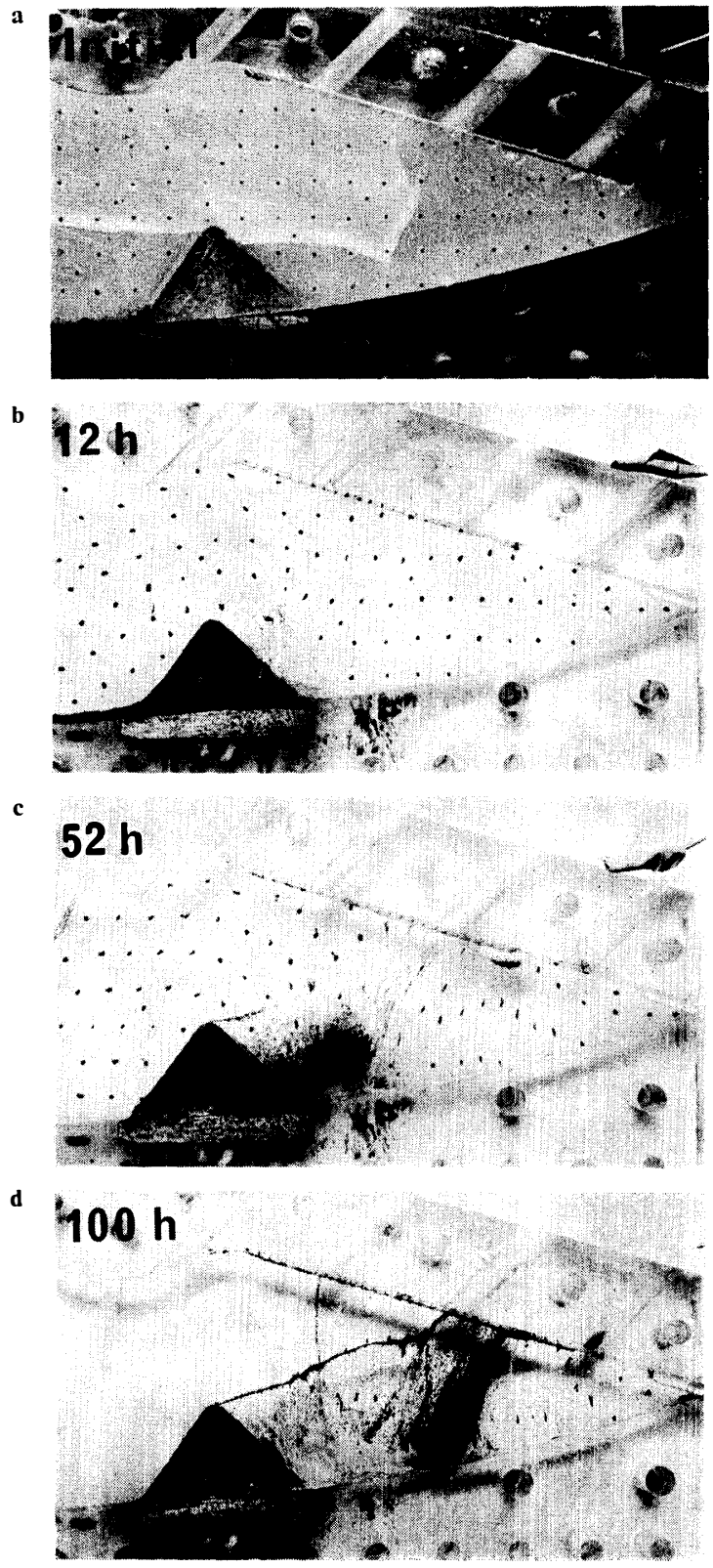

Fig. 3. Flow of ice and movement of sands in the experiment with the obstacle.

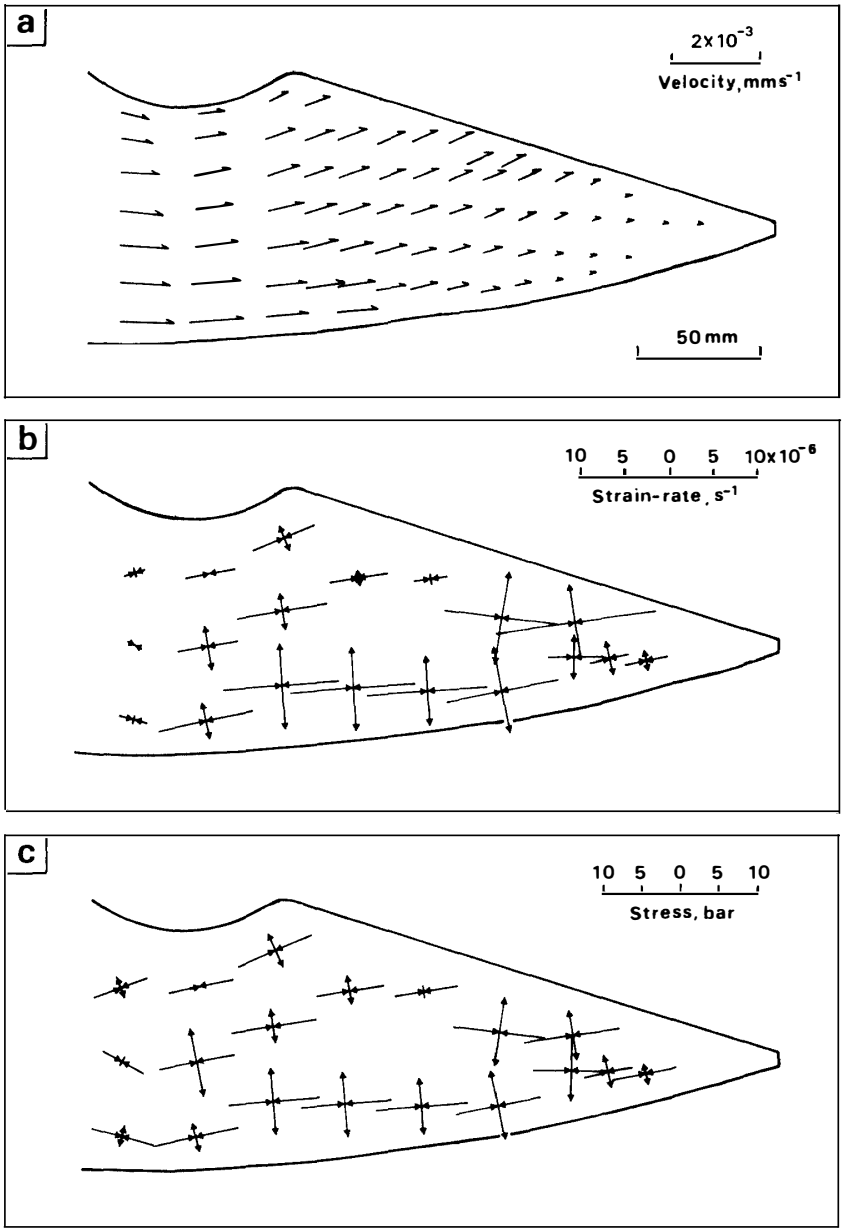

Fig. 4. The case of the smooth bed. (a) Velocity distribution. (b) Principal strain-rates. (c) Principal stress deviators.

where $\dot{\epsilon}_1$, $\dot{\epsilon}_2$, $\dot{\epsilon}_3$ are the principal strain-rates, and σ_1', σ_2', σ_3' are the principal stress deviators. Assuming that the flow of the form $\dot{e}=f(\tau)$ exists, NYE (1957) has shown that the stress deviators have the following relationship:

$$\sigma_i' = \frac{\tau}{\dot{e}} \dot{\epsilon}_i \quad (i=1, 2, 3). \tag{3}$$

The flow law given by GLEN's experiments (GLEN, 1955) for uniaxial compression at -0.02°C leads to

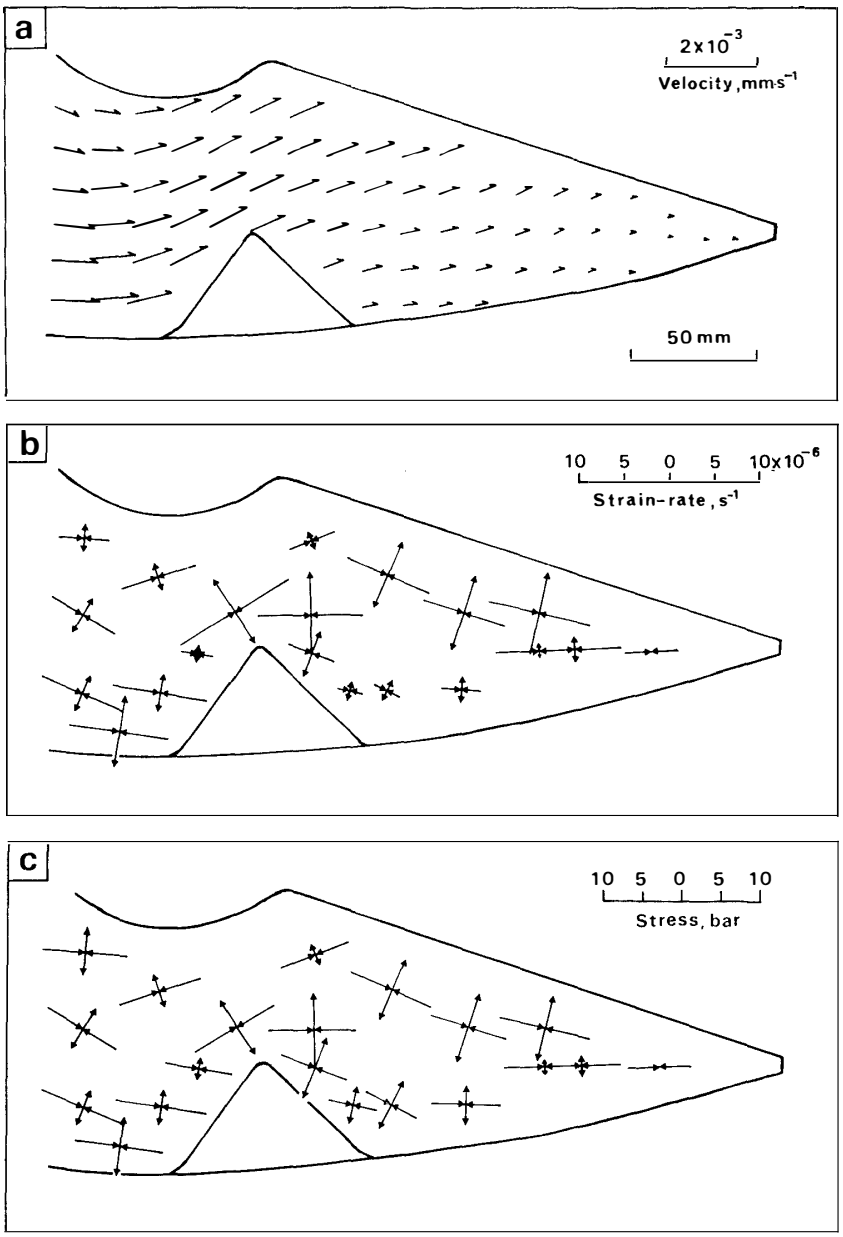

Fig. 5. The case of the bed with an obstacle. (a) Velocity distribution. (b) Principal strain-rates. (c) Principal stress deviators.

$$\dot{e} = 4.69 \times 10^{-9}\, \tau^{4.2}, \tag{4}$$

where $\dot{e}$ is in s^{-1} and τ is in bar. Using eqs. (3) and (4) the principal stress deviators are obtained by the equation:

$$\sigma_i' = 96.0\, \dot{e}^{-0.76}\, \dot{\varepsilon}_i \quad (i = 1, 2, 3). \tag{5}$$

The principal stress deviators calculated using eq. (5) are shown in Figs. 4c and 5c. The calculated results will be described below in detail.

3.2.1. The case of the smooth bed

As shown in Fig. 4a, the velocity of markers in the first five hours is large in the

upstream, but decreases considerably near the terminus. The velocity vector has an upward component in the middle stream, particularly near the upper surface. The velocity vector distribution shown in this figure indicates that the ice mass near the upper surface moves faster than that at the bottom and consequently the shear displacement takes place in the ice. Since the apparatus is devised so that the terminus ice does not melt and stays stagnant, the ice mass from upstream should be blocked by the stagnant ice zone, and rides over it.

Principal strain-rates shown in Fig. 4b indicate that the flow of ice is compressive. In the upstream and near the bottom, the principal compression axes are approximately parallel to the velocity vectors, but not necessarily so near the surface. Principal strain-rates are large in magnitude near the bed and in the immediate upstream of the stagnant ice zone, but small in the stagnant ice and near the upper surface in the midstream.

As shown in Fig. 4c, the magnitude of the compressive component of principal stress deviators is 5–6 bar near the bed and in the immediate upstream of the stagnant ice zone, but about 4 bar in the upper part and the stagnant zone. The difference between the maximum and the minimum value of principal strain-rates is due to the large number of power in the flow law of eq. (4).

3.2.2. The case of the bed with a triangular obstacle

It can be seen from the distribution of velocity vectors shown in Fig. 5a that the ice moves diagonally upward in the direction of the obstacle. It was observed that the ice mass was not only deformed, but also melted at the upstream face of the obstacle because of an excessive pressure on it. Part of meltwater refroze on the downstream side of the obstacle. Namely, regelation took place. The refrozen ice was free of air bubbles, having the smaller grain size than that of ice above it. During the deformation, a cavity (about 5 mm wide and 20 mm high) was formed on the downstream side of the obstacle because of the deficit of ice which had flowed downstream, but it was ultimately closed. At the downstream side of the obstacle the flow velocity is larger near the upper surface than that near the bottom and it is very small near the terminus. The difference in flow velocity indicates complex shear displacement in the ice.

The strain-rate pattern is rather complex around the obstacle, as shown in Fig. 5b. Principal strain-rates are large in magnitude near the top of the obstacle, and are considerably small at the downstream side of the obstacle. Compared with Fig. 4b, it can be seen that the principal strain-rates are larger in magnitude in the upstream side of the obstacle and near the upper surface of the downstream than the case of the smooth bed. This is due to the presence of the obstacle which resists the flow of ice. The magnitude of the compressive component of the principal stress deviator is about 5 bar in the upstream side, about 6 bar near the top, and about 4 bar at the downstream side of the obstacle, as shown in Fig. 5c.

3.3. Velocity of flow of the ice due to regelation

As stated above, the ice mass moved over the obstacle by the processes of regelation and enhanced plastic deformation of the ice mass. As shown in Fig. 3, the sand particles were incorporated into the ice mass immediately above the portion of regelation

ice on the downstream side of the obstacle. Therefore, the regelation process seems to be important in understanding the incorporation mechanism of sand particles. Before calculating the velocity of ice passing around the obstacle due to regelation, it is necessary to evaluate the velocity due to the enhanced plastic deformation, V_p, caused by increased stress on the upstream side of the obstacle. It is approximately expressed by the following equation:

$$V_p = \bar{\dot{e}}\, l. \tag{6}$$

Where $\bar{\dot{e}}$ is the average effective strain-rate in the upstream side of the obstacle, and l is the distance over which the obstacle causes an increase in deformation (PATERSON, 1981). The value of l can be deduced from the distribution of velocity and the magnitude of principal strain-rates in comparison with those in the case of the smooth bed. Substituting $\bar{\dot{e}} = (4.7 \pm 0.3) \times 10^{-6}\ \mathrm{s}^{-1}$ and $l = 70 \pm 8$ mm into eq. (6), the velocity due to the enhanced plastic deformation is obtained as $V_p = (3.3 \pm 0.6) \times 10^{-7}$ m/s. This value accounts for about 30% of the observed velocity in the upstream side of the obstacle. Therefore, the velocity of ice due to regelation accounts for about 70% of the observed velocity.

The velocity of ice due to regelation depends on a temperature difference, ΔT, between the upstream and the downstream face of an obstacle, thermal conductivity of the obstacle, k, and the size of the obstacle. The velocity due to regelation in the normal direction to the upstream face, V_R, is expressed by the following equation:

$$V_R = \frac{\dot{Q}}{LA\rho}, \tag{7}$$

where $\dot{Q}$ is the heat flow through the obstacle per unit time, L is the latent heat of fusion of ice, A is the area of the upstream face of the obstacle, ρ is the density of ice.

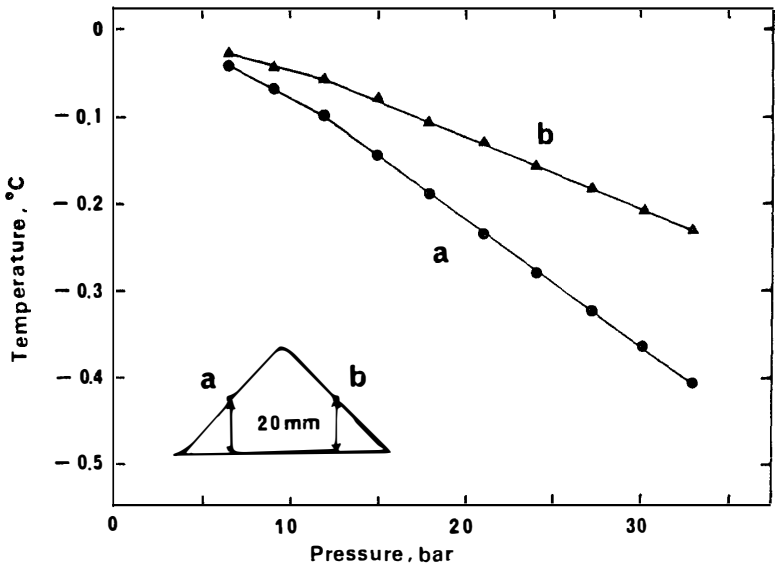

Fig. 6. Relationships between the load applied to the ice mass and the temperature at the upstream face (a) and the downstream face (b) of the obstacle.

To estimate the velocity of ice due to regelation, measurements were made of temperatures at the upstream and the downstream face of the obstacle as follows: Onto the upstream and the downstream face of the obstacle thermocouples were attached at a height of 20 mm above the base as shown in the lower left inset of Fig. 6. Temperatures at the two points (a) and (b) were measured as a function of compressive stress applied to the ice on the mouth of the mould. The results shown in Fig. 6 indicate that temperatures of both the upstream and the downstream face fall with increasing load. Since the falling rate of temperature on the upstream face is larger than that on the downstream face, the temperature difference between (a) and (b) increases with increasing load.

The velocity due to regelation was deduced by taking the temperature difference of 0.16°C for the pressure of 30 bar. It is assumed that the temperature is uniform on the upstream and the downstream face. Temperature distribution in the interior of the obstacle was then calculated by the iteration method, assuming the steady state of heat flow. Besides, the heat flow through the obstacle per unit time, $\dot{Q}$, was calculated from the temperature distribution, using the method of KATSUTOH (1964). Thus, $\dot{Q}=k\times 2.2\times 10^{-3}$ J/s, where the thermal conductivity, k, of the iron obstacle is 76 J/m·s·K. Inserting $\dot{Q}=1.67\times 10^{-1}$ J/s, $L=335$ kJ/kg, $A=8.4\times 10^{-4}$ m^2 and $\rho=890$ kg/m^3 in eq. (7) led to $V_R=6.7\times 10^{-7}$ m/s. This value accounts for 95% of the velocity in the normal direction to the upstream face of the obstacle calculated from the displacements of the marked points. The proportion of the velocity due to regelation calculated from temperature distribution to the total velocity does not agree with the proportion calculated from the strain-rates. The reason may be that the temperature at the face is not uniform. It calls for a need to measure temperature distributions at both the faces to make accurate calculation of regelation velocity.

4. Discussion and Concluding Remarks

4.1. Shear hypothesis

The present experiments disclosed that debris on the glacier bed are incorporated into the ice and form debris layers near the terminus, where stagnant ice zone exists. This suggests that the presence of the stagnant ice zone near the terminus plays an important role in the formation of inner moraines. Then, the question is whether or not such a stagnant ice zone exists at the bottom of a real glacier. As an answer, it is plausible to consider that it is formed at the boundary between the temperate and the cold ice at the bottom of the ice mass near the terminus where ice ceases to slide. The results of HOOKE's observation (HOOKE, 1973) on the stagnant wind-drift ice wedge may provide another answer.

As shown in Fig. 4, both longitudinal compression and shear displacement exist in the upstream of the stagnant ice zone, where principal strain-rates are large in magnitude. However, no discrete shear displacement was observed in the experiments. The experimental results suggest that, if there exists any shear displacement in ice due to the overriding of active ice on the stagnant ice zone, the debris on the bed can be incorporated into the ice mass without any discrete shear displacement.

4.2. Freezing model

In the experiments with the obstacle at the bottom, the sand particles were incorporated into the ice mass immediately above the portion of regelation ice to form a thin sand layer, and moved along the flow line to the upper surface (Fig. 3). This fact suggests that in nature, supposing many small bedrock obstacles exist, many debris layers can be formed from individual obstacle, as long as the materials of debris last. Probably a large number of slighty dirty ice layers can be formed.

The present experiments showed that a regelation process is important in the formation of inner moraines, and that the length and the thermal conductivity of obstacles are important in considering the regelation process under real glaciers. Observations at the base of Blue Glacier by KAMB and LACHAPELLE (1964) reported that the basal ice layer had smaller grains and contained much more dirt that the ice layers above it, and that the thickest part of the regelation layer is 3 cm in thickness. The present experiments showed that the velocity of ice due to regelation accounted for 95% of the velocity calculated from the displacements of the marked points. The iron obstacle, which was used in the experiments, has a higher thermal conductivity than rock materials. If the obstacle is made of dunite ($k=5.0$ J/m·s·K), the velocity of ice due to regelation will be 1/15 of the velocity obtained by the present experiments, which is smaller than the velocity due to the enhanced plastic deformation, V_p. Consequently, regelation will come to be effective in reality when a natural obstacle is smaller than 10 cm in length in the direction parallel to the flow line.

To sum up as a conclusion, the results of the present experiments conducted near 0°C suggest that debris can be incorporated into the ice mass by either shear action or regelation, and then move along the flow line upward to the surface. The results then support both the hypothesis of incorporation of debris by shear action and BOULTON's suggestion of the mechanism of incorporation of debris by basal freezing on the downstream side of a bedrock obstacle. Detailed mechanism of formation of inner moraines in natural glaciers is still to be studied.

Acknowledgments

The authors wish to thank Dr. K. TUSIMA, Toyama University, for his kind suggestions in their designing the experimental apparatus and carrying out the experiments. They are also grateful to the members of Applied Physics Section, the Institute of Low Temperature Science, Hokkaido University, for helpful discussions, and to anonymous referees for the refinement of the manuscript.

References

BISHOP, B. C. (1957): Shear moraines in the Thule area, northwest Greenland. SIPRE Res. Rep., **17**, 47p.

BOULTON, G. S. (1970): On the origin and transport of the englacial debris in Svalbard glaciers. J. Glaciol., **9**, 213–229.

GLEN, J. W. (1955): The creep of polycrystalline ice. Proc. R. Soc. London, Ser. **A, 228**, 519–538.

GOLDTHWAIT, R. P. (1951): Development of end moraines in east-central Baffin Island. J. Geol., **59**, 567–577.

GOLDTHWAIT, R. P. (1960): Study of ice cliff in Nunatarssuag, Greenland. SIPRE Tech. Rep., **39**, 108p.

HOLLIN, J. T. and CAMERON, R. L. (1961): I. G. Y. glaciological work at Wilkes Station, Antarctica. J. Glaciol., **3**, 833–842.

HOOKE, R. L. (1968): Comments on "The formation of shear moraines; An example from south Victoria Land, Antarctica". J. Glaciol., **7**, 351–352.

HOOKE, R. L. (1970): Morphology of the ice-sheet margin near Thule, Greenland. J. Glaciol., **9**, 303–324.

HOOKE, R. L. (1973): Flow near the margin of the Barnes Ice Cap, and the development of ice-cored moraines. Geol. Soc. Am. Bull., **84**, 3929–3948.

KAMB, B. and LACHAPELLE, E. R. (1964): Direct observation of the mechanism of glacier sliding over bedrock. J. Glaciol., **5**, 159–172.

KATSUTOH, Y. (1964): Dennetsu Gairon. Tokyo, Yôkendô, 453p.

NYE, J. F. (1953): The flow low of ice from measurements in glacier tunnels, laboratory experiments and Jungfraufirn borehole experiment. Proc. R. Soc. London, Ser. **A**, **219**, 477–489.

NYE, J. F. (1957): The distribution of stress and velocity in glaciers and ice sheets. Proc. R. Soc. London, Ser. **A**, **239**, 113–133.

NYE, J. F. (1959): A method of determining the strain-rate tensor at the surface of a glacier. J. Glaciol., **3**, 403–419.

PATERSON, W. S. B. (1981): The Physics of Glaciers. 2nd ed. Oxford, Pergamon, 380p.

SOUCHEZ, R. A. (1967): The formation of shear moraines; An example from south Victoria Land, Antarctica. J. Glaciol., **6**, 837–843.

SWINZOW, G. K. (1962): Investigation of shear zones in the ice-sheet margin, Thule area, Greenland. J. Glaciol., **4**, 215–229.

WARD, W. H. (1952): The glaciological studies of the Baffin Island Expedition, 1950. Part II: The physics of deglaciation in central Baffin Island. J. Glaciol., **2**, 9–23.

WEERTMAN, J. (1961): Mechanism for the formation of inner moraines found near the edge of cold ice caps and ice sheets. J. Glaciol., **3**, 965–978.

(Received April 25, 1983; Revised manuscript received July 18, 1983)